Desalination and Water Treatment
www.deswater.com
doi: 10.5004/dwt.2023.29932

310 (2023) 109–122
October

Hydrogen production from the hydrolysis of ammonia borane catalyzed by metal catalysts: a review

Jian Ren[a], Fengyan Xu[a], Jiaxin Ma[a], Yan Wang[a,b,*], Ke Zhang[a], Zhongqiu Cao[a], Qiuju Sun[a], Kezhen Qi[c], Guode Li[a,*], Shiwei Wu[a,*]

[a]*Institute of Catalysis for Energy and Environment, College of Chemistry and Chemical Engineering, Shenyang Normal University, Shenyang 110034, PR China, Tel.: 86-24-86576903; email: wangyan11287@mail.nankai.edu.cn (Y. Wang), Tel.: 86-24-86593318; email: liguode@synu.edu.cn (G. Li), Tel.: 86-24-86593318; emails: wsw@synu.edu.cn (S. Wu), 852917794@qq.com (J. Ren), 3120125723@qq.com (F. Xu), 2660649750@qq.com (J. Ma), 2694832243@qq.com (K. Zhang), caozhongqiu6508@sina.com (Z. Cao), sunqiuju@synu.edu.cn (Q. Sun)*
[b]*Key Laboratory of Advanced Energy Materials Chemistry (Ministry of Education), Nankai University, Tianjin 300071, PR China*
[c]*College of Pharmacy, Dali University, Dali 671000, Yunnan, China, email: qkzh2003@aliyun.com (K. Qi)*

Received 15 March 2023; Accepted 30 August 2023

ABSTRACT

As fossil fuels are gradually depleted, hydrogen energy is considered to be a replaceable energy on the world stage, which is mainly due to its high calorific value, small molecule and no pollution in combustion. However, there are still technical difficulties in hydrogen production and storage. Ammonia borane (NH_3BH_3) is a promising solid hydrogen storage material with good stable property and high hydrogen storage capacity of 19.6 wt.%. In this review, catalyzed hydrolysis of NH_3BH_3 by employed metal catalysts for hydrogen production is summarized, and its development direction is prospected to meet the future energy needs. There are two types of catalysts, containing non-supported catalysts and supported catalysts. By comparison, it can be inferred that supported catalysts show better catalytic activity toward the hydrolysis of NH_3BH_3. However, doping with non-noble metals is still commonly used, and the catalyzed mechanism about how the synergistic effect between metal nanoparticles and supports regulates the hydrolysis of NH_3BH_3 is further investigated. It will be more meaningful to develop new-style composite carriers, combine the theory and experiment to explore the catalytic activity and the mechanism of action, and exploit multi-component non-precious metal alloy supported catalysts.

Keywords: Ammonia borane; Hydrolysis; Hydrogen production; Metal catalysts

---

1. Introduction

Traditional fossil fuels, as non-renewable energy sources, have been unable to meet the energy needs of human production and life. The large amount of carbon dioxide produced by combustion has plagued human beings for many years [1,2]. Hydrogen energy is deemed to be in line with the goal of achieving carbon neutrality because of its advantages, including high calorific value, low carbon and environmental protection [3–5]. Consequently, many countries have incorporated hydrogen energy into national strategies [6–8]. In recent years, with the rapid development of chemical industry and technology, hydrogen can be obtained from hydrogen storage materials through various ways [9,10]. Therefore, it is especially important for the development of safe, environmentally friendly and efficient hydrogen production technology [11,12].

---

* Corresponding authors.

Ammonia borane (NH_3BH_3) has become a promising solid hydrogen storage material owing to good stable property and high hydrogen storage capacity of 19.6 wt.% [13,14]. The stored hydrogen can be released by pyrolysis, hydrolysis and alcoholysis [15–17]. Among them, the hydrolysis of NH_3BH_3 is a relatively simple, controllable and efficient strategy in the presence of suitable catalysts at room temperature [18]. The mechanism of the hydrolysis of NH_3BH_3 solution has been described by Xu and Chandra [19]. They have revealed that adsorbed NH_3BH_3 molecules on the catalyst surface firstly interacted with metals in aqueous solution to form active intermediates. Then, the attack of water molecules broke the B–N bond. Finally, the H in the water molecule combined with the H in the intermediate to form H_2. Based on the following hydrolysis reaction as presented in Eq. (1), it can be seen that 1 mol of NH_3BH_3 molecule can release 3 mol of hydrogen gas (H_2). Fig. 1 shows the corresponding mechanism of the H_2 released from the hydrolysis of NH_3BH_3 solution.

$$NH_3BH_3(aq) + 2H_2O \rightarrow NH_4BO_2(aq) + 3H_2(g) \qquad (1)$$

For the above-mentioned hydrolysis reaction, the investigation of low-cost and high-activity catalysts is significant to hydrogen generation. Nowadays, there are two types of reported catalysts toward the hydrolysis of NH_3BH_3, including non-supported and supported metal catalysts. In this review, we try to provide an overview of the recent advances in the field of metal catalysts for hydrogen generation from the hydrolysis of NH_3BH_3. The challenges and perspectives are discussed to further develop sustainable and clean hydrogen energy for its worldwide application in the future.

2. Non-supported catalyst

According to previous literatures, non-supported metal catalysts are directly used and are not attached to other carriers in chemical reactions, containing single metal and metal salt catalysts, transition metal phosphides, and metal alloys.

2.1. Single metal and metal salt catalysts

Single metal catalysts have attracted more and more concern because of the low cost, high abundance and variety in nature. It has been found that transition metals (such as Co, Ni, and Cu) have shown excellent catalytic performance in catalyzing the hydrolysis of NH_3BH_3. Yan et al. [20] synthesized amorphous Co nanoparticles *in-situ* at room temperature. By adjusting the molar ratio of Co and NH_3BH_3, the hydrogen from the hydrolysis of NH_3BH_3 can be completely released for 1.7 min. Subsequently, Qiu et al. [21] prepared Fe and Co nanoparticles, in which Co had higher catalytic activity. On the basis of single metal nanoparticles, a new structure was developed to enhance the catalytic activity. Ozay et al. [22] synthesized Co, Ni and Cu metal nanoparticles in the hydrogel network to catalyze NH_3BH_3 hydrolysis, and the activity decreased in the order of Co, Cu and Ni. Wei et al. [23] synthesized Ni hollow nanospheres by solvothermal reduction method. The corresponding transmission electron microscopy (TEM) images are displayed in Fig. 2a–c. The as-prepared catalysts showed high catalytic activity for NH_3BH_3 hydrolysis. Yao et al. [24] prepared Cu@SiO_2 core-shell nanoparticles by one-pot method in reversed-phase micelle system (Fig. 2d–f). The Cu@SiO_2 core-shell nanostructured catalyst has excellent catalytic activity for the hydrolysis of NH_3BH_3 to H_2 production at room temperature, which is better than that of single Cu nanoparticles and SiO_2 supported Cu nanoparticles.

Later, Sahiner and Alpaslan [25] successfully loaded metal salts in molecular form with water gel. The obtained p(APTMACl)-$[CuCl_4]^{2-}$ catalyst was employed to catalyze NH_3BH_3 hydrolysis under non-alkaline conditions, and its activation energy was close to that of the precious metal catalyst. Kalidindi et al. [26] reported that Co^{2+}, Ni^{2+} and Cu^{2+} could be used toward the hydrolysis of NH_3BH_3, and found that the performance of cobalt system was better than that of nickel and copper system.

2.2. Alloy catalysts

Alloy catalysts refer to the use of synergistic effects between metals and metals or metals and non-metals to form binary, ternary and even multi-component nanoparticles.

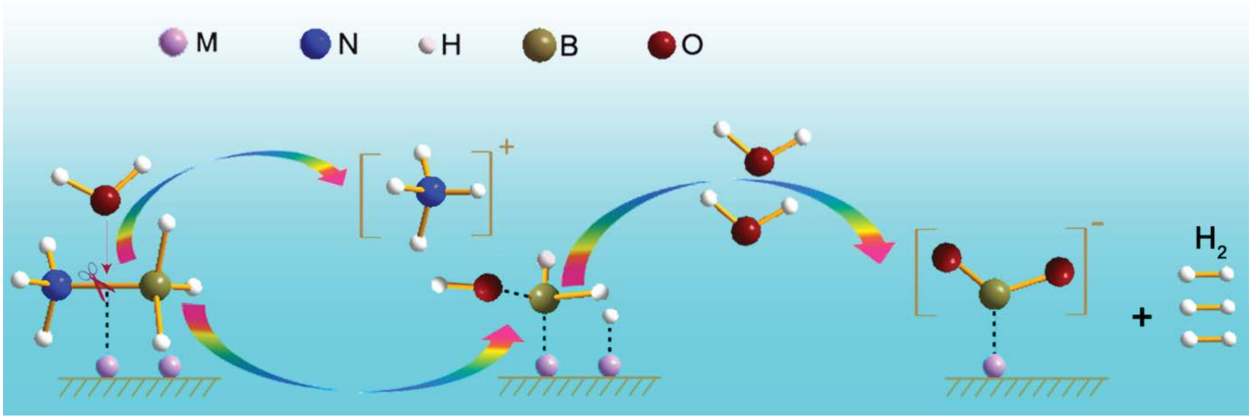

Fig. 1. Mechanism of the H_2 released from the hydrolysis of NH_3BH_3 solution.

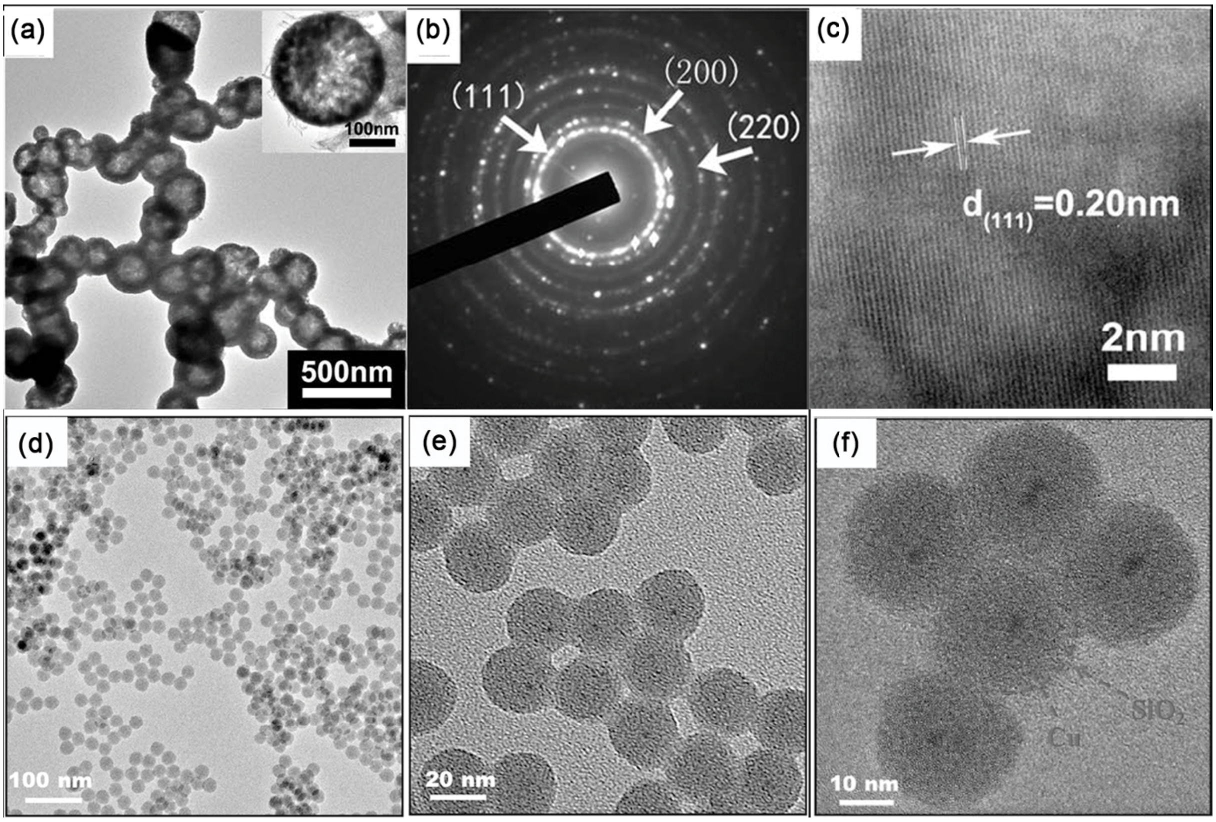

Fig. 2. (a) TEM, (b) SAED image, (c) HRTEM image of nickel hollow nanospheres [23], (d–f) TEM images of the Cu@SiO_2 core-shell nanospheres [24].

Compared with single-metal nanoparticles, alloy catalysts can show better catalytic activity and enhanced stability. Wang et al. [27] synthesized $Cu_{0.2}Co_{0.8}$ nanoparticles (NPs) supported on hierarchically porous carbon (HPC) for NH_3BH_3 hydrolysis. It possessed the high catalytic performance with the H_2 generation rate of 2,960 mL·min^{-1}·g^{-1}. Qiu et al. [21] *in-situ* synthesized FeCo catalysts with different proportions by a chemical reduction method. Among them, the catalytic activity of $Fe_{0.3}Co_{0.7}$ is best, displaying the lowest activation energy of 16.30 kJ·mol^{-1}. Kantürk Figen [28] prepared Co-B, Ni-B and Cu-B catalysts. They found that the catalytic activity was gradually weakened in turn. Fernandes et al. [29] obtained quaternary amorphous alloy Co-Mo-B-P by chemical reduction method, in which Mo, in the form of oxide, not only provided an atomic barrier to reduce the agglomeration rate of Co-B nanoparticles, but also provided Lewis acid sites to enhance the absorption of reactants. P could produce more Co active sites on the catalyst surface. After the co-doping of the two metals with Co-B, the catalytic performance was greatly improved when compared with Co-Mo-B, Co-B-P and Co-B alloy catalysts. Patel et al. [30] studied the high activity of nanoparticle-assembled Co-B catalyst. They found that the electrons of alloying B would transfer to vacant d-orbital of metallic Co, protecting Co from being oxidized and achieving efficiently catalytic hydrolysis of NH_3BH_3.

In addition to Co-based catalysts, Cu-based catalysts also have demonstrated good activity. Lu et al. [31] *in-situ* prepared a series of new $Cu_{1-x}Fe_x$ alloy nanoparticles. Fig. 3a–c give the representative TEM images of prepared $Cu_{0.33}Fe_{0.67}$ NPs. In particular, the catalytic performance of $Cu_{0.33}Fe_{0.67}$ NPs not only exceeded that of single metal NPs, but also exceeded that of $Cu_{0.33}$@$Fe_{0.67}$ core-shell NPs, and could still show high activity after 8 cycles as shown in Fig. 3d. Qiu et al. [32] reported Cu@FeCo core-shell NPs with Cu as core and FeCo as shell. From Fig. 3e–f it can be seen that the particle size of $Cu_{0.3}$@$Fe_{0.1}Co_{0.6}$ NPs was about 10–15 nm. The energy-dispersive X-ray (EDX) spectrum in Fig. 3g verified the existence of Cu, Fe and Co. The obtained $Cu_{0.3}$@$Fe_{0.1}Co_{0.6}$ with the highest Co content had the best performance with the lower E_a value of 38.75 kJ·mol^{-1} (Fig. 3h), showing that the regulation of metal ratio significantly improved the synergistic effect between Cu, Fe and Co. Wang et al. [33] prepared Cu@MoCo core-shell NPs, Cu, Cu@Co and Cu@Mo. According to the TEM images and size distributions in Fig. 4a–d, it was found that the addition of Mo greatly reduced the agglomeration of the catalysts. Moreover, the high catalytic activity toward the hydrolysis of NH_3BH_3 was obtained (Fig. 4e and f). From the previous reports, it can be concluded that co-deposition of various elements has made the catalyst particle size smaller and more uniform, and effectively improved the efficiency of NH_3BH_3 hydrolysis, indicating that the catalytic activity of multi-component alloys have been enhanced.

The catalytic effect of Ni-based alloys is also very outstanding. Yan et al. [34] prepared a series of FeNi alloys

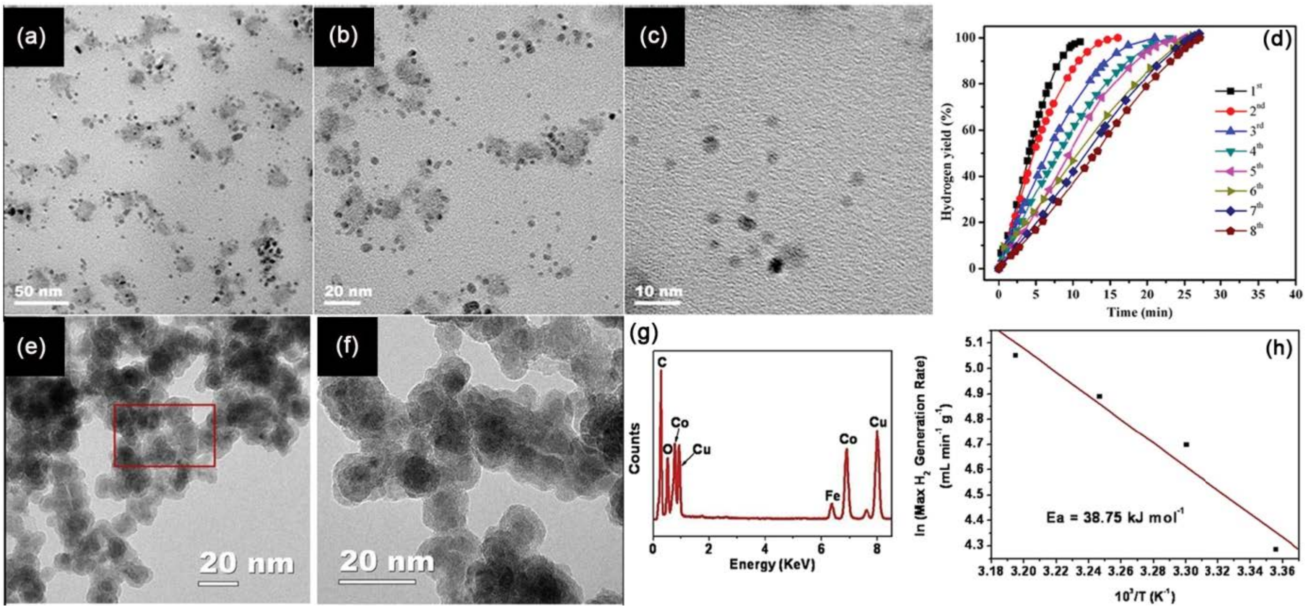

Fig. 3. Representative TEM images (a–c) scale bars from left to right: 50, 20, 10 nm and the reusability after 8 cycles for the prepared $Cu_{0.33}Fe_{0.67}$ nanoparticles [31]. (e,f) TEM and (g) EDX spectrum (the marked area of e) for $Cu_{0.3}@Fe_{0.1}Co_{0.6}$ core-shell NPs, and (h) Arrhenius plot (ln*k* vs. (1/*T*)) for the hydrolysis of NH_3BH_3 in the presence of $Cu_{0.3}@Fe_{0.1}Co_{0.6}$ core-shell NPs [32].

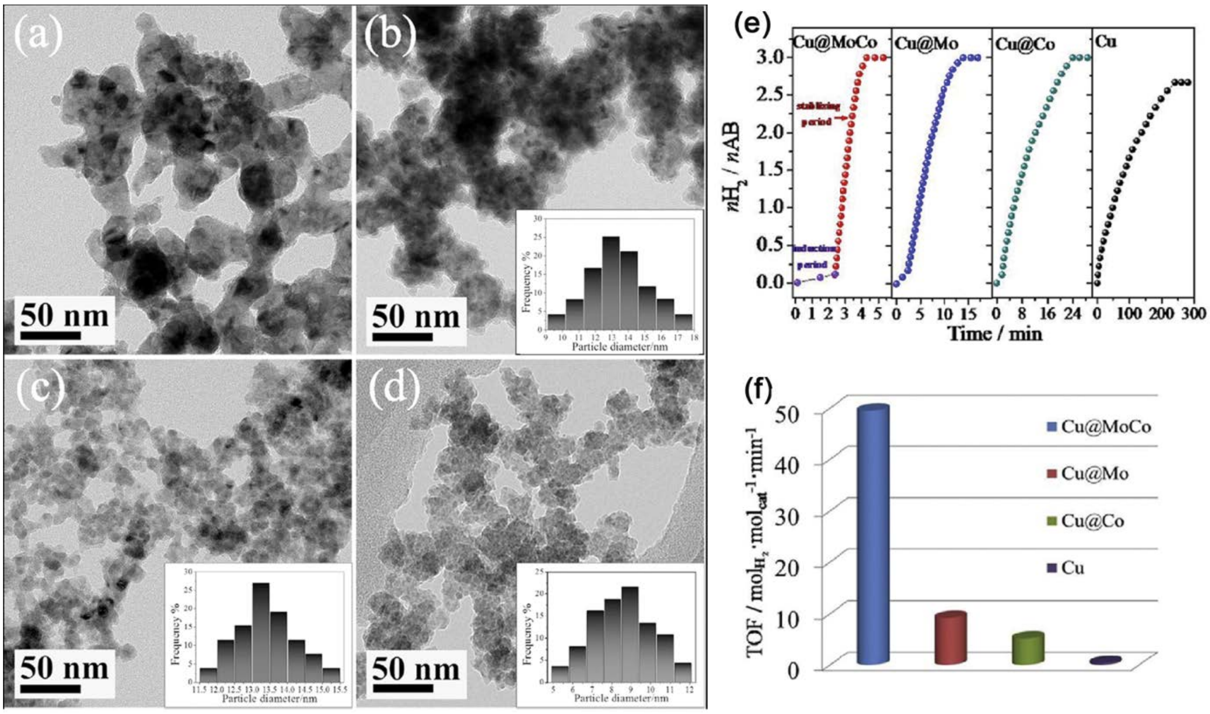

Fig. 4. TEM images and the corresponding size distributions of (a) Cu, (b) Cu@Co, (c) Cu@Mo, (d) Cu@MoCo NPs and (d,f) kinetics curve and TOF values for the hydrolytic dehydrogenation of NH_3BH_3 catalyzed by Cu@MoCo, Cu@Mo, Cu@Co, and Cu NPs [33].

with different ratios. Especially for the $Fe_{0.5}Ni_{0.5}$ catalyst, it exhibited the catalytic activity similar to Pt in the process of the NH_3BH_3 hydrolysis. Du et al. [35] also manufactured FeNi alloys and discovered that the activity was the best when the molar ratio of Fe and Ni was 1, which was consistent with Yan's research results. On this basis, Ni-Pt nanoparticles were obtained by doping a small amount of Pt. They observed that the catalytic hydrogen release time was shortened by half, and the activation energy was also lower, indicating that doping noble metal into non-noble metal to form alloys can enhance the activity of the non-noble metal-based catalyst.

2.3. Transition metal phosphide catalysts

The transition metal phosphide can transfer electrons to the P center through the metal. Due to the electron-donating effect of the metal and the aggregation effect of P, the NH_3BH_3 molecule has a strong adsorption function, which effectively activates the B–N bond in NH_3BH_3, thereby reducing the reaction energy barrier and achieving the purpose of accelerating H_2 evolution. The transition metal phosphide has been extensively studied in recent years.

Feng et al. [36] synthesized Ni_2P and Ni_5P_4 to catalyze the hydrolysis of NH_3BH_3 by phase-controlled thermal decomposition for the hydrolysis of NH_3BH_3. Theoretical calculations and experimental data confirmed that Ni_5P_4 had better catalytic performance. It was found that the more electrons transferred from Ni to P, the better the effect of catalyzing NH_3BH_3 hydrolysis, further illustrating that those electron-donating catalysts performed better than the electron-accepting catalysts. Wan et al. [37] prepared CoP and Co_2P nanoparticles. The discovered that low P content of Co_2P reduced the electron transfer from Co to P, making the charge distribution more uniform (Fig. 5a–f). Moreover, the d band center of Co_2P had stronger adsorption on intermediate products than CoP (Fig. 5c and f), showing the better catalytic performance. Peng et al. [38] prepared FeP, Cu_3P and Ni_2P, and the corresponding catalytic activity was enhanced successively. In addition, the results showed that the catalytic activity of small particles Ni_2P was higher than that of large particles at the initial stage (Fig. 5g–i). Based the above-mentioned reports, it can be seen that transition metal phosphides have excellent performance in catalyzing the hydrolysis of NH_3BH_3 to H_2 production, and the catalyst activity can be enhanced by further adjusting the diameter of nanoparticles.

Compared with bulk materials, the catalytic effect of non-supported catalysts is significantly improved, but catalyst nanoparticles are generally easy to agglomerate, resulting in the rapid degradation of catalytic performance and short cycle life [39].

3. Supported catalyst

In view of the deficiencies of non-supported catalysts, supported catalysts have been gradually attracted attention. After loading precious metals, non-precious metals or alloys, they can greatly enhance the stability of the catalyst, reduce the agglomeration rate, and improve the catalytic activity. At present, the catalysts commonly used in catalyzing NH_3BH_3 hydrolysis to hydrogen production are supported by oxide supports, carbon-based supports, metal–organic frameworks (MOFs) supports and other supports.

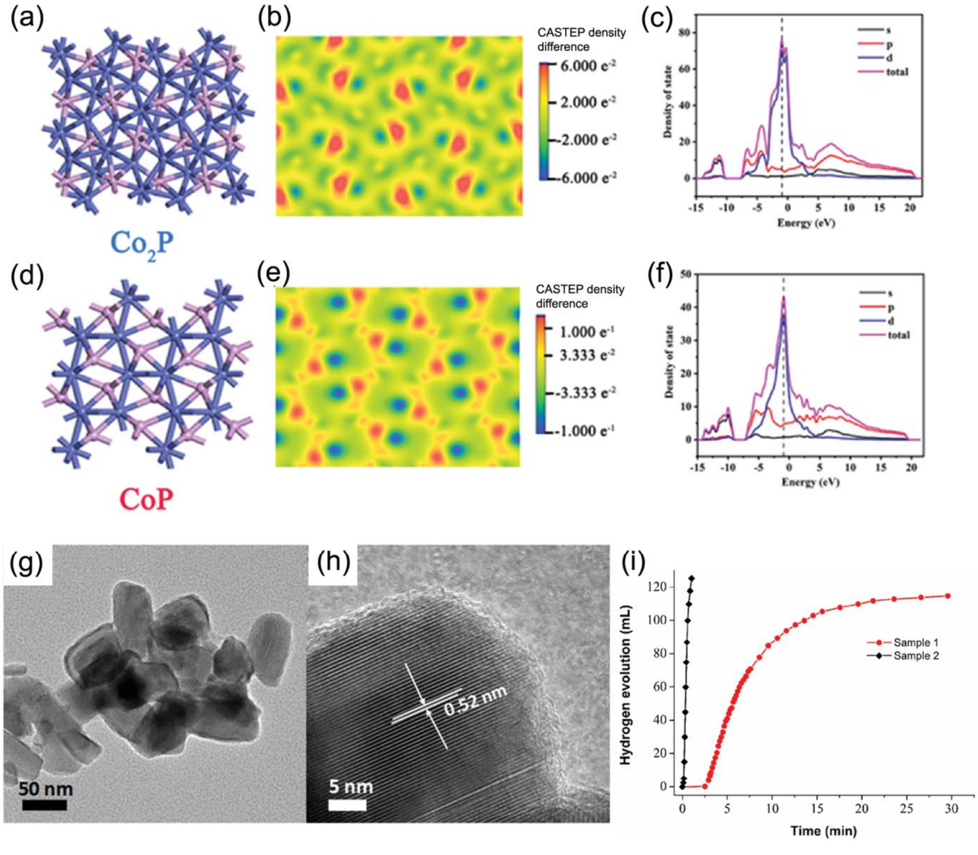

Fig. 5. (a,d) Structure, (b,e) corresponding charge density distribution and (c,f) DOS plots of Co_2P and CoP, respectively [37], (g) TEM, (h) HRTEM images of Ni_2P NP sample and (i) the H_2 evolution over time in water (5 mL) containing NH_3BH_3 (1.62 mmol) and Ni_2P (0.259 mmol) at 298 K [38].

3.1. Oxide supports

The strong interaction between the oxide and the metal makes the metal particles more dispersed, which greatly reduces the attenuation of catalyst performance due to agglomeration [40–42]. Hence, some oxides are usually used as the carrier of catalytic materials because of their catalytic effects on the hydrolysis of NH_3BH_3 [43–48].

Akbayrak et al. [47] investigated the effect of different oxide supports (CeO_2, SiO_2, Al_2O_3, TiO_2, ZrO_2, HfO_2) on the catalytic activity of Rh NPs toward the hydrolysis of NH_3BH_3. They found that Rh attached to nanopowders of CeO_2 showed higher catalytic activity. Subsequently, the research group [49] anchored Co, Ni, Cu and Fe on nano CeO_2 by impregnation reduction method, and the order of catalytic activity was Co > Ni > Cu > Fe. Zhou and Xu [46] fabricated nanoporous (NP) $PtCo/Co_3O_4$ composites with different Pt/Co ratios, which significantly improved the catalytic performance for NH_3BH_3 hydrolysis, especially NP-$Pt_{40}Co_{60}$ complex (Fig. 6a and b), in which the surface-anchored Co_3O_4 nanosheets exhibited higher catalytic activity with a high TOF value of 131 min^{-1} (Fig. 6c). Wu et al. [43] adopted an especial approach instead of using Co_3O_4 as a carrier and successfully synthesized Co-Co_3O_4 powders with different degrees of oxidation. It was found that Co-Co_3O_4 was more active than the mixture of Co and Co_3O_4 (Fig. 6d). Considering that the introduction of Co_3O_4 changed the electronic structure of Co, the water molecules adsorbed on Co_3O_4 dissociated to form OH* radicals bonded to surface Co atoms and H atoms bonded to the neighbouring O atoms. It can be inferred that the interface will accumulate a large number of H* atoms and OH* radicals, which not only contributes to the generation of H_2 molecules by increasing the collision probability between H* atoms, but also promotes the progress of S_{N2} reaction and increase the reaction rate (Fig. 6e).

In view of the above-mentioned reports, it can be discovered that the different metal supported by the same oxide support shows different catalytic activity. The interactions between the metal and the support, and even between the metal nanoparticles, have various degrees of influence on the catalytic performance. Except for the above oxide supports, the common ones are Fe_3O_4 [50], $CoFe_2O_4$ [51], TiO_2 [52], and so on. In addition, Feng et al. [53] obtained Cu_2O-CoO nanoplate composite catalyst after simple hydrothermal synthesis and calcination. Compared with the NH_3BH_3 hydrolysis catalyzed by Cu_2O and CoO nanoparticles, the TOF value of Cu_2O-CoO was about 10 times higher. In the two-dimensional element mapping analysis, it was found that Cu, Co and O were evenly distributed. All these indicate that there is a strong synergistic effect between Cu_2O and CoO, which greatly enhances the activity and stability of the composite catalyst.

Based on the previous reports, it can be seen that the oxide supports show good catalytic performance in catalyzing NH_3BH_3 hydrolysis. To further refine the catalytic activity, there are some strategies can be adopted, such as the construction of binary, ternary and even multi-element

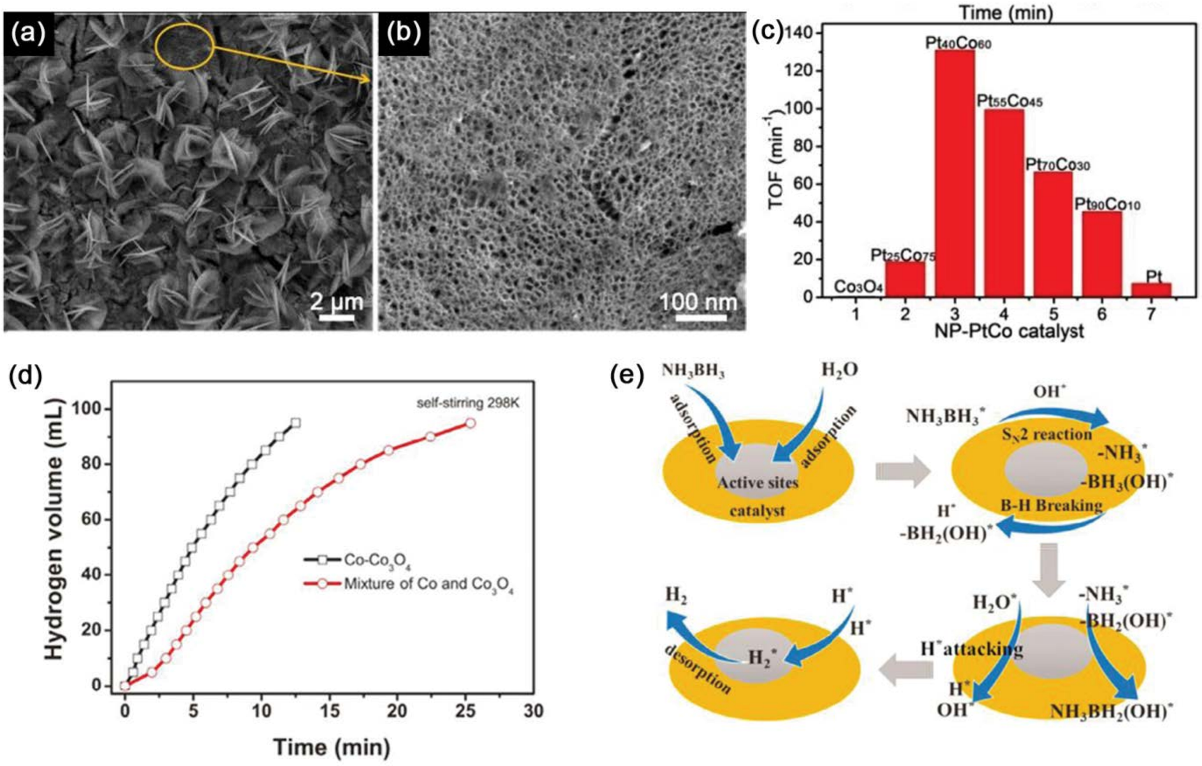

Fig. 6. (a,b) SEM images of NP-$Pt_{40}Co_{60}$, and (c) TOF values vs. amount of Pt in the NP-PtCo/Co_3O_4 catalyst [46], (d) comparison of Co-Co_3O_4, Co and Co_3O_4 NPs mixtures for the hydrolysis of NH_3BH_3 and (e) schematic diagram of hydrogen generation process of NH_3BH_3 hydrolysis under appropriate catalyst [43].

alloys, using the interaction between metal nanoparticles, selecting oxide supports with appropriate specific surface area. Besides, the development of new catalysts with distinctive structures, wherein oxides are not restricted to be used as carriers, but also as active components, providing new ideas for the synthesis prospects of supported catalysts.

3.2. Carbon-based materials as carriers

3.2.1. Graphene support

In recent years, graphene has become a hot research topic owing to its large specific surface area, unique physicochemical property, and nearly transparent structure [54]. Wang et al. and Ke et al. [55,56] prepared Co@rGO and Co-Mo@rGO composite catalysts with a bayberry-like structure by adding surfactant PVA, controlling the preparation process and adding graphene support. Among them, bayberry fruit Co-Mo nanoparticles had better structure, better dispersion, and smaller particle size on the graphene surface. Compared with single metal particles, the interface synergy between bimetallic particles and carriers of Co-Mo@rGO could effectively improve the dispersion and stability, showing the better catalytic activity. Zou et al. [57] obtained graphene-supported Co-CeO_x catalyst by a facile impregnation and chemical reduction method. They pointed out that the catalytic activity of Co-CeO_x/graphene was significantly higher than that of pure Co and Co/graphene, which might be due to the addition of the oxide support, contributing to the dispersion of Co nanoparticles and leading to the enhancement the catalytic activity. Moreover, they also explored the effect of other transition metal oxides on the catalytic performance, based on the order of Yb > Er > Ce > Dy > Tb > La.

Fig. 7a and b show the comparison of reported TOF and E_a values for various non-noble based catalysts with graphene support toward the NH_3BH_3 hydrolysis [58–64], respectively. It can be seen that the graphene-supported catalyst has been improved when compared with single metal, but the TOF value is still not high, and the catalytic effect is not ideal for satisfying the application requirement. To effectively improve the catalytic activity, the graphene loading, preparation method, and technological parameter remain to be further explored.

3.2.2. Porous carbon support

Porous carbon material has a large specific surface area, which is conducive to the adequate contact between the catalyst and the reactants. Especially, its large pore size can disperse metal nanoparticles and reduce the deactivation caused by agglomeration. On this basis, porous nitrogen and nonmetal-doped carbon (such as N-C, B-C and O-C, etc.) are gradually formed and employed as the catalyst supports [15,65].

Zou et al. [66] loaded Co-Ni-B on porous activated carbon, and the TOF value was as high as 1,451.2 $mL^{-1}\cdot min^{-1}\cdot g^{-1}$. Wang et al. [27] used HPC as support and prepared $Cu_{0.2}Co_{0.8}$ NPs on HPC ($Cu_{0.2}Co_{0.8}$/HPC) with high surface area of 600 $m^2\cdot g^{-1}$. The TEM images in Fig. 8a and b display that $Cu_{0.2}Co_{0.8}$ NPs were homogenously dispersed on HPC with the mean sizes of 8.2 nm. The line scanning analysis from Fig. 8c presented the element of Cu and Co in the NPs was very homogenously distributed. In Fig. 8d–f the hydrogen generation kinetics shows that the catalytic activity was significantly better than that of $Cu_{0.2}Co_{0.8}$ nano-alloy particles, and its dispersibility was still relatively good after repeated hydrogen desorption. They also used Co (salen) as the precursor to prepare Co@N-C nanocomposites by high temperature calcination. The catalytic effect is lower than that of $Cu_{0.2}Co_{0.8}$/HPC, but the catalytic activity can still maintain 97.2% after multiple cycles. Yuan et al. [15] constructed a 3D mesoporous spherical assembled by N-doped carbon coated Ni/Pd NP heterojunctions (Ni/Pd@N-C) (Fig. 9a). The unique structure afforded a relative large surface area and exposing high fractions of active sites as shown in Fig. 9b–g. Moreover, utilizing the synergistic effect between Ni and Pd, and the coating of N-doped carbon, the catalytic activity was

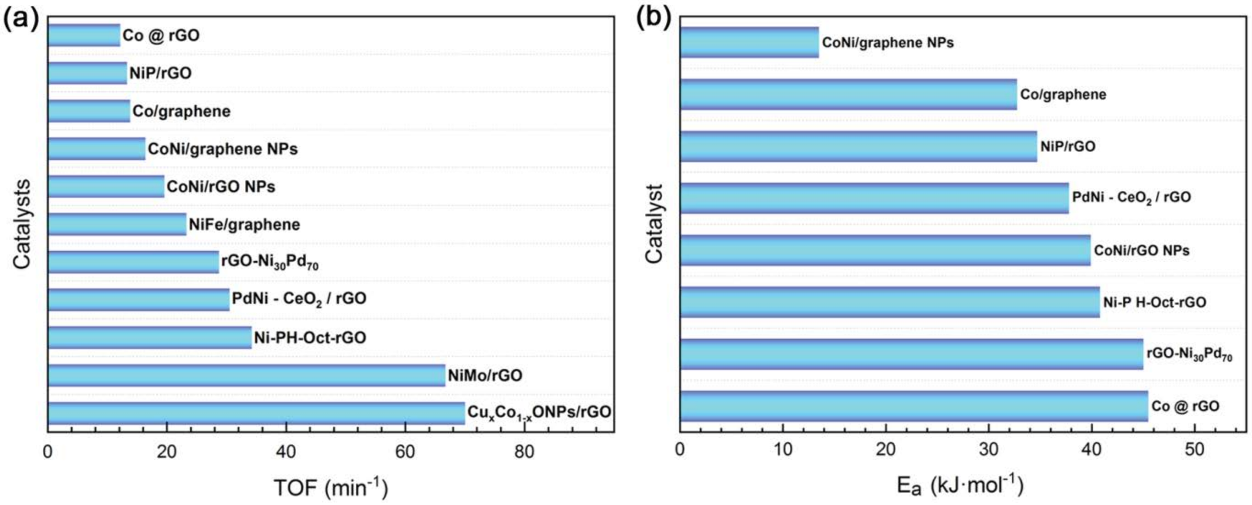

Fig. 7. Comparison of reported TOF (a) and E_a (b) values for various non-noble based catalysts with graphene support toward the NH_3BH_3 hydrolysis.

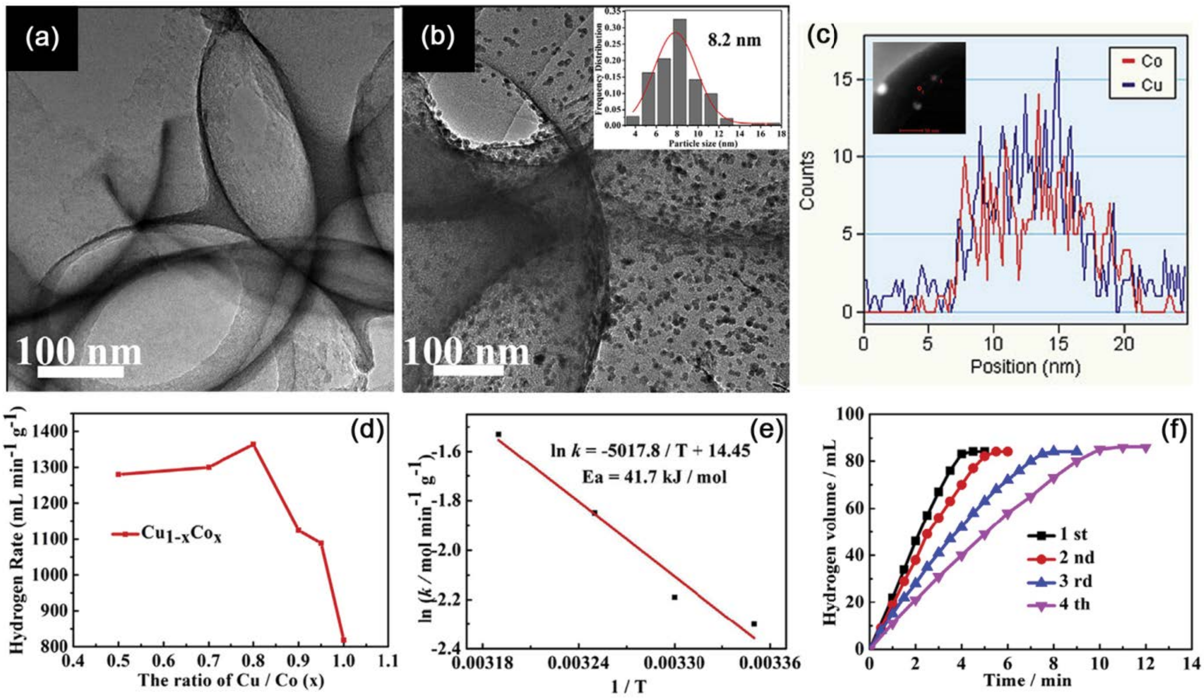

Fig. 8. (a,b) TEM images of HPC and $Cu_{0.2}Co_{0.8}$/HPC, (c) line scanning analysis and (inset) dark-field TEM image $Cu_{0.2}Co_{0.8}$/HPC, (d) effect of the Co content on hydrogen generation rate of NH_3BH_3, (e) corresponding Arrhenius plot and (f) the recyclability of 32.3 wt.% $Cu_{0.2}Co_{0.8}$/HPC in catalyzing the hydrolytic hydrogen generation of NH_3BH_3, respectively [27].

well balanced and improved as exhibited in Fig. 9h and i, containing the stability and recyclability.

Except for nitrogen doping, Qu et al. [65] also explored the properties of oxygen-doped carbon supports and supported ternary NiCoP alloys on them. The prepared noble-metal-free $Ni_{0.66}Co_{0.19}P_{0.15}$/OPC nanocatalyst showed superior catalytic activity with the TOF value of 95.24 min^{-1}. On the basis of binary doped carbon supports, Xu et al. [67] supported Co-Mo and Co-W on boron-nitrogen-doped porous carbon nanospheres, and the obtained activation energy was lower than most of the reported catalysts (such as Ni/C, Co/N-C, $CoRu_x$/N-C, $Ni_{0.66}Co_{0.19}P_{0.15}$/OPC, $Cu_{0.2}Co_{0.8}$/HPC).

3.2.3. Graphitic carbon nitride support

Graphitic carbon nitride (g-C_3N_4) is a mental-free two-dimensional polymer semiconductor material. It can be synthesized from urea, melamine and other raw materials by pyrolysis or other simple methods [68–70]. Recently, g-C_3N_4 has got a lot of attention due to its superior photocatalytic activity in hydrogen generation. Hence, it is considered as a kind of carrier to stabilize active metal-based nanoparticles. Although the reports about noble metals supported on g-C_3N_4 are easily found [71–73], there is very little research on non-precious metals supported on g-C_3N_4. Gao et al. [74] anchored monodisperse Ni nanoparticles on g-C_3N_4 with different size by a self-assembly route as listed in Fig. 10a–c. The noble-mental-free Ni/g-C_3N_4 showed excellent photocatalytic performance toward the catalytic dehydrogenation from NH_3BH_3 under visible light (Fig. 10d and e), providing the TOF value of 18.7 min^{-1} and apparent E_a value of 36 kJ·min^{-1}. Based on the special structure and composition, they supplied the reaction mechanism as shown in Fig. 10f, revealing that the electron could rapidly transfer to the Ni NPs through the interface between g-C_3N_4 and Ni NPs. Li et al. [75] synthesized $Cu_{0.4}Co_{0.6}MoO_4$ rod-like nanocatalysts dispersed on g-C_3N_4. The TOF value was much higher than that of the unsupported $Cu_{0.4}Co_{0.6}MoO_4$ and single metal supported on g-C_3N_4.

3.3. MOFs support

MOFs materials are composed of organic ligands combined with inorganic metal ions or clusters through self-assembly method. Its characteristics mainly include large specific surface area, adjustable pore size, and structural modifiability [76,77]. The organic framework structure can effectively reduce the agglomeration of metal nanoparticles and form a unique interfacial synergy [78]. Recent research suggests that the catalytic activity and stability can be greatly enhanced after metals are supported on MOFs. Gao et al. [79] adhered Cu and Ni to MIL-101 by liquid-phase impregnation method, and found that the prepared Cu_2Ni_1/MIL-101 catalyst had excellent catalytic performance with TOF value of 20.9 min^{-1} after adjusting the ratio of Cu to Ni. Li and Li [80] manufactured binary AgCo/MIL-101 and ternary CuFeCo/MIL-101 via an easy impregnation-reduction process. Liang et al. [81] synthesized $Cu_{0.8}Ni_{0.1}Co_{0.1}$/MIL-101 by solvent evaporation. Yang et al. [82] also prepared RuCuCo/MIL-101 catalyst by liquid-phase impregnation method. Compared with the binary alloys, the ternary alloys displayed good catalytic activity for the dehydrogenation from NH_3BH_3 hydrolysis because of the high dispersion of the trimetallic nanoparticles in MIL-101. After

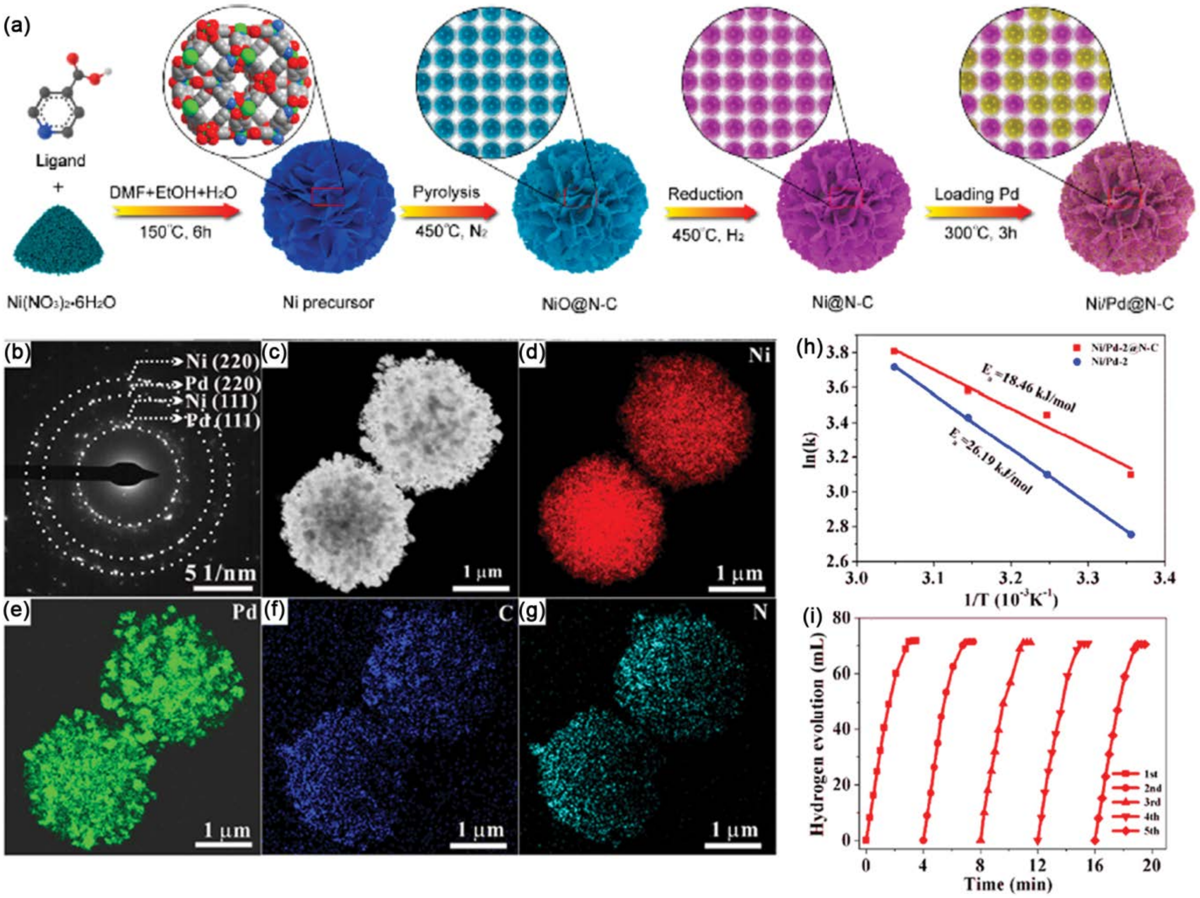

Fig. 9. (a) Schematic illustration of the preparation process of Ni/Pd@N-C hierarchical mesoporous sphere, (b) SAED pattern and (c–g) STEM image and EDX elemental mapping of Ni/Pd-2@N-C mesoporous spheres, (h) Arrhenius plots for NH_3BH_3 hydrolysis by employing Ni/Pd-2@N-C and Ni/Pd-2 catalysts and (f) cycle stability of Ni/Pd-2@N-C catalyst [15].

multiple cycles, the stability was well maintained, which could be attributed to the good support and synergy of the MOFs. On the basis of the adding of Cu, Co, Fe, Ni and Ru, it could be inferred that the addition of noble metals made the TOF value of the supported catalyst significantly higher than that of non-precious metals according to the comparison as drawn in Fig. 11a, but the E_a value was also relatively high. In addition to MIL-101, MIL-like MOFs also include MIL-96 [83,84] and MIL-53 [85]. The introduction of precious metals is commonly employed as a part of the MOFs supported catalyst to achieve the high catalytic activity. However, for the single precious metal catalyst supported by MIL-53, the addition of non-precious metals reduces the catalytic activity as shown in Fig. 11b.

Li et al. [86] first immobilized uniformly dispersed Ni NPs on ZIF-8 to catalyze hydrolysis of NH_3BH_3. They revealed that the catalytic process occurred on the metal surface, and the NH_3BH_3 molecules interacted with the surface of the metal particles to form an activated complex. ZIF-8 effectively controlled the Ni NPs into the smaller particle size range and increased the surface area, exhibiting high catalytic activity and durability toward NH_3BH_3 hydrolysis. Wang et al. [87] synthesized zeolite imidazolite skeleton structure material ZIF-67@Co by *in-situ* Mosaic reduction method. The TOF value was 112.3 mol·mol^{-1}·min^{-1}, and the activity retained 92% after seven cycles, which showed that its catalytic performance was much higher than that of Co NPs. Zhou et al. [77] incorporated Pd-doped Cu NPs into the interior of ZIF-67/ZIF-8 ($CuPd_{0.01}$@ZIF-67@ZIF-8) by a double-solvent approach. The confinement of the core-shell layer resulted in the ultrafine size (~3 nm) of metal nanoparticles and the combination of Pd and Cu. The synergistic effect between them made it show excellent activity for the hydrogen generation from NH_3BH_3 hydrolysis. It can be concluded that MOFs can support metal nanoparticles well. However, the emphasis is on how to utilize the synergistic effect between multi-component non-noble metal alloys and novel MOFs to improve the catalytic performance of supported catalysts without noble metal doping.

3.4. Other materials as carriers

Sun et al. [39] developed a new strategy by using TiO_2-CdS nanotubes (TCNTs) as a support to load metal NPs. They prepared Cu/TCNTs nanocatalysts for the hydrolysis of NH_3BH_3 with a high TOF value of 3.8 min^{-1}. Zhou et al. [88] and Zhao et al. [89] used the hydrothermal method to synthesize NiCo LDH (layered double hydroxide) and

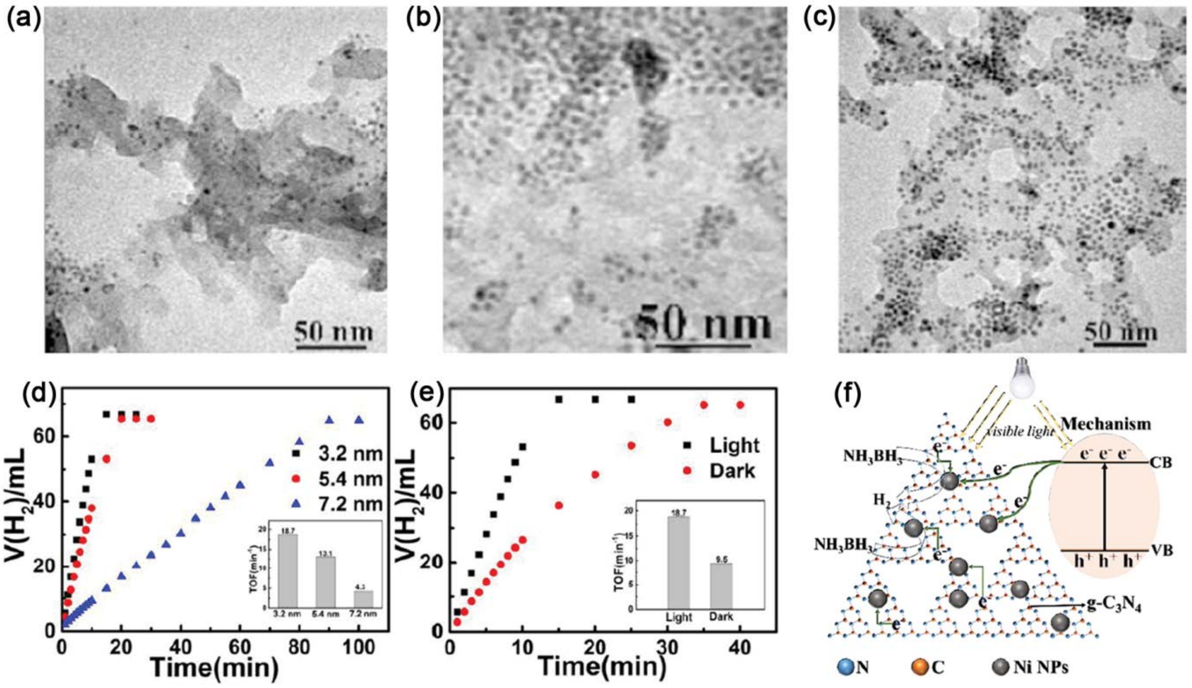

Fig. 10. (a–c) TEM images of the Ni NPs with different sizes, (d) plot of the hydrogen generation kinetics for NH_3BH_3 hydrolysis catalyzed by Ni/g-C_3N_4 catalysts with different Ni NPs sizes under visible light irradiation, (e) plot of the hydrogen generation kinetics catalyzed by 3.2 nm Ni/g-C_3N_4 and (f) corresponding schematic of photocatalytic NH_3BH_3 hydrolysis under visible light irradiation [74].

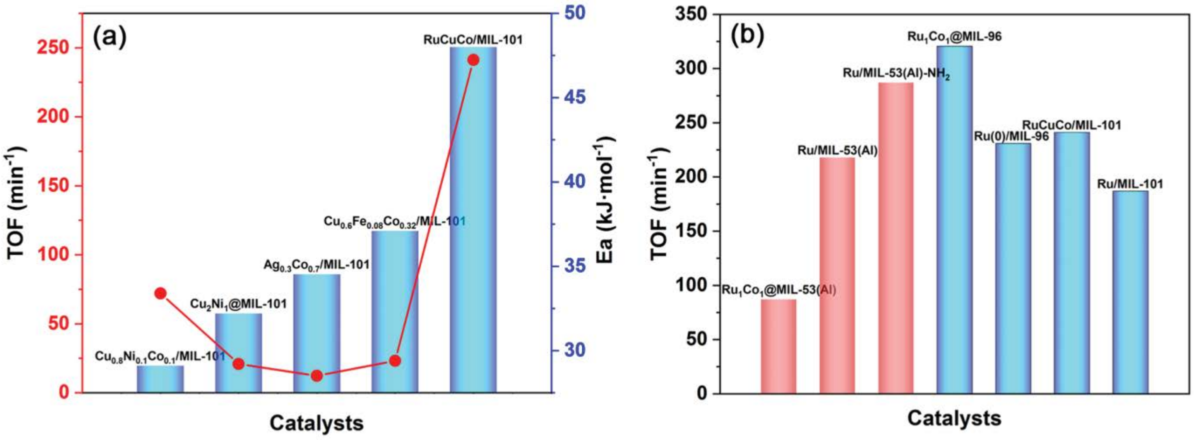

Fig. 11. (a) Comparison of TOF value and E_a of multi-alloy nanocatalyst with MIL-101 as carrier and (b) comparison of TOF values of noble metal catalysts and the doped non-noble metal catalysts with MOFs materials as carrier.

Mg_2Al-LDH-h layered double metal hydroxide supports, respectively. They are all employed to load the noble metals, but the catalytic activity is not ideal, which needs to be further explored.

Paladini et al. [90] used the magnetron sputtering method to support Co on the Ni foam for the first time, and prepared a highly active amorphous Co/Ni foam catalyst by controlling the time and pressure. Later, Wang et al. [91] introduced Cu foil as a substrate to load Co-Mo-B catalyst by chemical deposition method, and the catalyzed hydrogen generation rate from NH_3BH_3 hydrolysis was 5818 mL·min^{-1}·g^{-1}. In addition, thin-film Co-W-P/Cu foam, Co-Ni-B/Cu foil, and Co-W-B/foam sponge catalysts were also obtained by electroless plating method. They showed the novel nanostructure with regular small particles and large specific surface area.

A variety of carriers mainly play the role of supporting and dispersing catalyst nanoparticles. Moreover, some carriers themselves also have a certain catalytic effect on the hydrolysis of NH_3BH_3. Research suggests that electron transfer can effectively improve catalyst activity, so it is much meaningful to develop the carriers for electron transfer between them and catalysts in the future, which can protect the supported catalysts from oxidation and further improve catalyst performance.

4. Summary and outlook

In conclusion, we have reviewed the types of metal catalyzed NH_3BH_3 hydrolysis for hydrogen production, containing non-supported catalysts and supported catalysts. It can be seen that supported catalysts show better catalytic performance than non-supported catalysts. Among them, several carriers can effectively support and disperse metal nanoparticles, and even catalyze the hydrolysis of NH_3BH_3. The catalysts with high activity are still doped with non-noble metals. However, the mechanism of how the synergistic effect between metal nanoparticles and supports regulates the hydrolysis of NH_3BH_3 needed to be further investigated. Different supports often have a great influence on the catalytic activity.

In the future, we can try to develop new-style composite carriers based on core-shell structures, metal-metal oxides and alloys, combine the theory and experiment to explore the catalytic activity and the mechanism of action for the non-precious supported metal nanoparticles with different particle sizes. On this basis, exploiting multi-component non-precious metal alloy catalysts to replace precious metals will be particularly important.

Acknowledgments

This work was supported by National Natural Science Foundation of China (22075186, 21975164), Key Laboratory of Advanced Energy Materials Chemistry (Ministry of Education) (111 project, B12015), the Natural Science Foundation of Liaoning Province (2022-MS-310), the Scientific Research Fund of Liaoning Provincial Education Department (LJKZ0993), the Revitalization Talents Program (XLYC1907013) of Liaoning Province, Liaoning BaiQianWan Talents Program (2021921091), the Science and Technology Project of Shenyang (21-108-9-05), the Hundred Talent Program and Major Incubation Project (ZD202003) of Shenyang Normal University.

Declarations

Conflict of interest

The authors declare that they have no conflict of interest.

Data and code availability

The data that support the findings of this study are available from the corresponding author.

Supplementary information

Not applicable

Ethical approval

Not applicable

References

[1] R. Shen, Y. Liu, H. Wen, T. Liu, Z. Peng, X. Wu, X. Ge, S. Mehdi, H. Cao, E. Liang, J. Jiang, B. Li, Engineering V_O-Ti ensemble to boost the activity of Ru towards water dissociation for catalytic hydrogen generation, Appl. Catal., B, 306 (2022) 121100, doi: 10.1016/j.apcatb.2022.121100.

[2] K. Qi, C. Zhuang, M. Zhang, P. Gholami, A. Khataee, Sonochemical synthesis of photocatalysts and their applications, J. Mater. Sci. Technol., 123 (2022) 243–256.

[3] X.-J. Fang, L.-P. Ren, F. Li, Z.-X. Jiang, Z.-G. Wang, Modulating electronic structure of $CoSe_2$ by Ni doping for efficient electrocatalyst for hydrogen evolution reaction, Rare Met., 41 (2022) 901–910.

[4] C. Li, J. Zhou, W. Gao, J. Zhao, J. Liu, Y. Zhao, M. Wei, D.G. Evans, X. Duan, Binary Cu–Co catalysts derived from hydrotalcites with excellent activity and recyclability towards NH_3BH_3 dehydrogenation, J. Mater. Chem. A, 1 (2013) 5370–5376.

[5] A. Kantürk Figen, M.B. Pişkin, B. Coşkuner, V. İmamoğlu, Synthesis, structural characterization, and hydrolysis of ammonia borane (NH_3BH_3) as a hydrogen storage carrier, Int. J. Hydrogen Energy, 38 (2013) 16215–16228.

[6] W. Cheng, S. Lee, How green are the national hydrogen strategies?, Sustainability, 14 (2022) 1930, doi: 10.3390/su14031930.

[7] A.B. Burg, H.I. Schlesinger, Hydrides of boron. VII. Evidence of the transitory existence of borine (BH_3): borine carbonyl and borine trimethylammine, J. Am. Chem. Soc., 59 (1937) 780–787.

[8] F. Li, J. Li, L. Chen, Y. Dong, P. Xie, Q. Li, Preparation of CoB nanoparticles decorated PANI nanotubes as catalysts for hydrogen generation from $NaBH_4$ hydrolysis, J. Taiwan Inst. Chem. Eng., 122 (2021) 148–156.

[9] C. Wang, Q. Wang, F. Fu, D. Astruc, Hydrogen generation upon nanocatalyzed hydrolysis of hydrogen-rich boron derivatives: recent developments, Acc. Chem. Res., 53 (2020) 2483–2493.

[10] M.L. Meena, K. Kumar, P. Saini, M. Sethi, S. Saini, A. Mohapatra, S. Som, R.-Y. Lin, C.-W. Chu, C.-H. Lu, S.D. Lin, V. Parewa, Competent production of hydrogen and hydrogenation of carboxylic acids using urea-rich waste water over visible-light-responsive rare earth doped photocatalyst, J. Taiwan Inst. Chem. Eng., 144 (2023) 104734, doi: 10.1016/j.jtice.2023.104734.

[11] Z. Li, W. Wang, Q. Qian, Y. Zhu, Y. Feng, Y. Zhang, H. Zhang, M. Cheng, G. Zhang, Magic hybrid structure as multifunctional electrocatalyst surpassing benchmark Pt/C enables practical hydrazine fuel cell integrated with energy-saving H_2 production, eScience, 2 (2022) 416–427.

[12] Y.M. Shi, B. Zhang, Recent advances in transition metal phosphide nanomaterials: synthesis and applications in hydrogen evolution reaction, Chem. Soc. Rev., 45 (2016) 1529–1541.

[13] C. Wang, X. Yu, X. Zhang, Z. Lu, X. Wang, X. Han, J. Zhao, L. Li, X. Yang, Enhanced hydrogen production from ammonia borane over CuNi alloy nanoparticles supported on TiO_2(B)/anatase mixed-phase nanofibers with high specific surface area, J. Alloys Compd., 815 (2020) 152431, doi: 10.1016/j.jallcom.2019.152431.

[14] S.G. Shore, R.W. Parry, The crystalline compound ammonia-borane, NH_3BH_3, J. Am. Chem. Soc., 77 (1955) 6084–6085.

[15] Y. Yuan, L. Sun, G. Wu, Y. Yuan, W. Zhan, X. Wang, X. Han, Engineering nickel/palladium heterojunctions for dehydrogenation of ammonia borane: improving the catalytic performance with 3D mesoporous structures and external nitrogen-doped carbon layers, Inorg. Chem., 59 (2020) 2104–2110.

[16] L. Cui, Y.H. Xu, L. Niu, W.R. Yang, J.Q. Liu, Monolithically integrated CoP nanowire array: an on/off switch for effective on-demand hydrogen generation via hydrolysis of $NaBH_4$ and NH_3BH_3, Nano Res., 10 (2017) 595–604.

[17] T. Umegaki, J.M. Yan, X.B. Zhang, H. Shioyama, N. Kuriyama, Q.A. Xu, Co-SiO_2 nanosphere-catalyzed hydrolytic dehydrogenation of ammonia borane for chemical hydrogen storage, J. Power Sources, 195 (2010) 8209–8214.

[18] D. Lim, G. Özkan, G. Özkan, Ni-B and Zr–Ni–B *in-situ* catalytic performance for hydrogen generation from sodium borohydride, ammonia borane and their mixtures, Int. J. Hydrogen Energy, 47 (2022) 3396–3408.

[19] Q. Xu, M. Chandra, Catalytic activities of non-noble metals for hydrogen generation from aqueous ammonia–borane at room temperature, J. Power Sources, 163 (2006) 364–370.

[20] J.-M. Yan, X.-B. Zhang, H. Shioyama, Q. Xu, Room temperature hydrolytic dehydrogenation of ammonia borane catalyzed by Co nanoparticles, J. Power Sources, 195 (2010) 1091–1094.

[21] F.Y. Qiu, Y.J. Wang, Y.P. Wang, L. Li, G. Liu, C. Yan, L.F. Jiao, H.T. Yuan, Dehydrogenation of ammonia borane catalyzed by *in-situ* synthesized Fe–Co nano-alloy in aqueous solution, Catal. Today, 170 (2011) 64–68.

[22] O. Ozay, E. Inger, N. Aktas, N. Sahiner, Hydrogen production from ammonia borane via hydrogel template synthesized Cu, Ni, Co composites, Int. J. Hydrogen Energy, 36 (2011) 8209–8216.

[23] W. Wei, Z. Wang, J. Xu, L. Zong, K. Zhao, H. Wang, H. Li, R. Yu, Cobalt hollow nanospheres: controlled synthesis, modification and highly catalytic performance for hydrolysis of ammonia borane, Sci. Bull., 62 (2017) 326–331.

[24] Q. Yao, Z.-H. Lu, Z. Zhang, X. Chen, Y. Lan, One-pot synthesis of core-shell Cu@SiO_2 nanospheres and their catalysis for hydrolytic dehydrogenation of ammonia borane and hydrazine borane, Sci. Rep., 4 (2014) 7597, doi: 10.1038/srep07597.

[25] N. Sahiner, D. Alpaslan, Metal-ion-containing ionic liquid hydrogels and their application to hydrogen production, J. Appl. Polym. Sci., 131 (2014) 40183, doi: 10.1002/app.40183.

[26] S.B. Kalidindi, M. Indirani, B.R. Jagirdar, First row transition metal ion-assisted ammonia-borane hydrolysis for hydrogen generation, Inorg. Chem., 47 (2008) 7424–7429.

[27] H. Wang, L. Zhou, M. Han, Z. Tao, F. Cheng, J. Chen, CuCo nanoparticles supported on hierarchically porous carbon as catalysts for hydrolysis of ammonia borane, J. Alloys Compd., 651 (2015) 382–388.

[28] A. Kantürk Figen, Dehydrogenation characteristics of ammonia borane via boron-based catalysts (Co-B, Ni-B, Cu-B) under different hydrolysis conditions, Int. J. Hydrogen Energy, 38 (2013) 9186–9197.

[29] R. Fernandes, N. Patel, A. Miotello, L. Calliari, Co–Mo–B–P alloy with enhanced catalytic properties for H_2 production by hydrolysis of ammonia borane, Top. Catal., 55 (2012) 1032–1039.

[30] N. Patel, R. Fernandes, G. Guella, A. Miotello, Nanoparticle-assembled Co-B thin film for the hydrolysis of ammonia borane: a highly active catalyst for hydrogen production, Appl. Catal., B, 95 (2010) 137–143.

[31] Z.-H. Lu, J. Li, A. Zhu, Q. Yao, W. Huang, R. Zhou, R. Zhou, X. Chen, Catalytic hydrolysis of ammonia borane via magnetically recyclable copper iron nanoparticles for chemical hydrogen storage, Int. J. Hydrogen Energy, 38 (2013) 5330–5337.

[32] F. Qiu, Y. Dai, L. Li, C. Xu, Y. Huang, C. Chen, Y. Wang, L. Jiao, H. Yuan, Synthesis of Cu@FeCo core–shell nanoparticles for the catalytic hydrolysis of ammonia borane, Int. J. Hydrogen Energy, 39 (2014) 436–441.

[33] C. Wang, H. Wang, Z. Wang, X. Li, Y. Chi, M. Wang, D. Gao, Z. Zhao, Mo remarkably enhances catalytic activity of Cu@MoCo core-shell nanoparticles for hydrolytic dehydrogenation of ammonia borane, Int. J. Hydrogen Energy, 43 (2018) 7347–7355.

[34] J.-M. Yan, X.-B. Zhang, S. Han, H. Shioyama, Q. Xu, Magnetically recyclable Fe–Ni alloy catalyzed dehydrogenation of ammonia borane in aqueous solution under ambient atmosphere, J. Power Sources, 194 (2009) 478–481.

[35] J. Du, F. Cheng, M. Si, J. Liang, Z. Tao, J. Chen, Nanoporous Ni-based catalysts for hydrogen generation from hydrolysis of ammonia borane, Int. J. Hydrogen Energy, 38 (2013) 5768–5774.

[36] X. Feng, Y. Zhao, D. Liu, Y. Mo, Y. Liu, X. Chen, W. Yan, X. Jin, B. Chen, X. Duan, D. Chen, C. Yang, Towards high activity of hydrogen production from ammonia borane over efficient non-noble Ni_5P_4 catalyst, Int. J. Hydrogen Energy, 43 (2018) 17112–17120.

[37] C. Wan, Y. Liang, L. Zhou, J. Huang, J. Wang, F. Chen, X. Zhan, D.-g. Cheng, Integration of morphology and electronic structure modulation on cobalt phosphide nanosheets to boost photocatalytic hydrogen evolution from ammonia borane hydrolysis, Green Energy Environ., (2022), doi: 10.1016/j.gee.2022.06.007 (in Press).

[38] C.Y. Peng, L. Kang, S. Cao, Y. Chen, Z.S. Lin, W.F. Fu, Nanostructured Ni_2P as a robust catalyst for the hydrolytic dehydrogenation of ammonia–borane, Angew. Chem. Int. Ed., 54 (2015) 15725–15729.

[39] D. Sun, Y. Hao, C. Wang, X. Zhang, X. Yu, X. Yang, L. Li, Z. Lu, W. Shang, TiO_2–CdS supported CuNi nanoparticles as a highly efficient catalyst for hydrolysis of ammonia borane under visible-light irradiation, Int. J. Hydrogen Energy, 45 (2020) 4390–4402.

[40] H. Cao, W. Wang, T. Cui, H. Wang, G. Zhu, X. Ren, Enhancing CO_2 hydrogenation to methane by Ni-Based catalyst with V species using 3D-mesoporous KIT-6 as support, Energies, 13 (2020) 2235, doi: 10.3390/en13092235.

[41] W. Li, X. Nie, X. Jiang, A. Zhang, F. Ding, M. Liu, Z. Liu, X. Guo, C. Song, ZrO_2 support imparts superior activity and stability of Co catalysts for CO_2 methanation, Appl. Catal., B, 220 (2018) 397–408.

[42] Y. Lv, C. Han, Y. Zhu, T. Zhang, S. Yao, Z. He, L. Dai, L. Wang, Recent advances in metals and metal oxides as catalysts for vanadium redox flow battery: properties, structures, and perspectives, J. Mater. Sci. Technol., 75 (2021) 96–109.

[43] H. Wu, M. Wu, B. Wang, X. Yong, Y. Liu, B. Li, B. Liu, S. Lu, Interface electron collaborative migration of Co–Co_3O_4/carbon dots: boosting the hydrolytic dehydrogenation of ammonia borane, J. Energy Chem., 48 (2020) 43–53.

[44] J. Zhu, L. Ma, J. Feng, T. Geng, W. Wei, J. Xie, Facile synthesis of Cu nanoparticles on different morphology ZrO_2 supports for catalytic hydrogen generation from ammonia borane, J. Mater. Sci.: Mater. Electron., 29 (2018) 14971–14980.

[45] D.R. Abd El-Hafiz, G. Eshaq, A.E. ElMetwally, Recent enhancement of ammonia borane hydrolysis using spinel-type metal ferrites nano-catalysts, Mater. Chem. Phys., 217 (2018) 562–569.

[46] Q. Zhou, C. Xu, Nanoporous PtCo/Co_3O_4 composites with high catalytic activities toward hydrolytic dehydrogenation of ammonia borane, J. Colloid Interface Sci., 508 (2017) 542–550.

[47] S. Akbayrak, Y. Tonbul, S. Özkar, Ceria supported rhodium nanoparticles: superb catalytic activity in hydrogen generation from the hydrolysis of ammonia borane, Appl. Catal., B, 198 (2016) 162–170.

[48] A. Yousef, N.A.M. Barakat, M.H. El-Newehy, M.M. Ahmed, H.Y. Kim, Catalytic hydrolysis of ammonia borane for hydrogen generation using Cu(0) nanoparticles supported on TiO_2 nanofibers, Colloids Surf., A, 470 (2015) 194–201.

[49] S. Akbayrak, O. Taneroğlu, S. Özkar, Nanoceria supported cobalt(0) nanoparticles: a magnetically separable and reusable catalyst in hydrogen generation from the hydrolysis of ammonia borane, New J. Chem., 41 (2017) 6546–6552.

[50] Y. Guo, J. Qian, A. Iqbal, L. Zhang, W. Liu, W. Qin, Pd nanoparticles immobilized on magnetic carbon dots@Fe_3O_4 nanocubes as a synergistic catalyst for hydrogen generation, Int. J. Hydrogen Energy, 42 (2017) 15167–15177.

[51] Y. Tonbul, S. Akbayrak, S. Özkar, Magnetically separable rhodium nanoparticles as catalysts for releasing hydrogen from the hydrolysis of ammonia borane, J. Colloid Interface Sci., 553 (2019) 581–587.

[52] A. Yousef, N.A.M. Barakat, K.A. Khalil, A.R. Unnithan, G. Panthi, B. Pant, H.Y. Kim, Photocatalytic release of hydrogen from ammonia borane-complex using Ni(0)-doped TiO_2/C electrospun nanofibers, Colloids Surf., A, 410 (2012) 59–65.

[53] Y. Feng, H. Wang, X. Chen, F. Lv, Y. Li, Y. Zhu, C. Xu, X. Zhang, H.-R. Liu, H. Li, Simple synthesis of Cu_2O–CoO nanoplates with enhanced catalytic activity for hydrogen production

from ammonia borane hydrolysis, Int. J. Hydrogen Energy, 45 (2020) 17164–17173.

[54] B. Zhao, J. Liu, L. Zhou, D. Long, K. Feng, X. Sun, J. Zhong, Probing the electronic structure of M-graphene oxide (M = Ni, Co, NiCo) catalysts for hydrolytic dehydrogenation of ammonia borane, Appl. Surf. Sci., 362 (2016) 79–85.

[55] J. Wang, D. Ke, Y. Li, H. Zhang, C. Wang, X. Zhao, Y. Yuan, S. Han, Efficient hydrolysis of alkaline sodium borohydride catalyzed by cobalt nanoparticles supported on three–dimensional graphene oxide, Mater. Res. Bull., 95 (2017) 204–210.

[56] D. Ke, Y. Tao, Y. Li, X. Zhao, L. Zhang, J. Wang, S. Han, Kinetics study on hydrolytic dehydrogenation of alkaline sodium borohydride catalyzed by Mo-modified Co-B nanoparticles, Int. J. Hydrogen Energy, 40 (2015) 7308–7317.

[57] A. Zou, X. Xu, L. Zhou, L. Lin, Z. Kang, Preparation of graphene-supported Co-CeO$_x$ nanocomposites as a catalyst for the hydrolytic dehydrogenation of ammonia borane, J. Fuel Chem. Technol., 49 (2021) 1371–1378.

[58] C. Cui, Y. Liu, S. Mehdi, H. Wen, B. Zhou, J. Li, B. Li, Enhancing effect of Fe-doping on the activity of nano Ni catalyst towards hydrogen evolution from NH_3BH_3, Appl. Catal., B, 265 (2020) 118612, doi: 10.1016/j.apcatb.2020.118612.

[59] X. Zhao, D. Ke, S. Han, Y. Li, H. Zhang, Y. Cai, Reduced graphene oxide sheets supported waxberry-like Co catalysts for improved hydrolytic dehydrogenation of ammonia borane, ChemistrySelect, 4 (2019) 2513–2518.

[60] L. Yang, N. Cao, C. Du, H. Dai, K. Hu, W. Luo, G. Cheng, Graphene supported cobalt(0) nanoparticles for hydrolysis of ammonia borane, Mater. Lett., 115 (2014) 113–116.

[61] Y.-H. Zhou, Z. Zhang, S. Wang, N. Williams, Y. Cheng, S. Luo, J. Gu, rGO supported PdNi-CeO$_2$ nanocomposite as an efficient catalyst for hydrogen evolution from the hydrolysis of NH_3BH_3, Int. J. Hydrogen Energy, 43 (2018) 18745–18753.

[62] R. Zhang, J. Zheng, T. Chen, G. Ma, W. Zhou, RGO-wrapped Ni-P hollow octahedrons as noble-metal-free catalysts to boost the hydrolysis of ammonia borane toward hydrogen generation, J. Alloys Compd., 763 (2018) 538–545.

[63] W. Feng, L. Yang, N. Cao, C. Du, H. Dai, W. Luo, G. Cheng, *In-situ* facile synthesis of bimetallic CoNi catalyst supported on graphene for hydrolytic dehydrogenation of amine borane, Int. J. Hydrogen Energy, 39 (2014) 3371–3380.

[64] N.S. Çiftci, Ö. Metin, Monodisperse nickel–palladium alloy nanoparticles supported on reduced graphene oxide as highly efficient catalysts for the hydrolytic dehydrogenation of ammonia borane, Int. J. Hydrogen Energy, 39 (2014) 18863–18870.

[65] X. Qu, R. Jiang, Q. Li, F. Zeng, X. Zheng, Z. Xu, C. Chen, J. Peng, The hydrolysis of ammonia borane catalyzed by NiCoP/OPC-300 nanocatalysts: high selectivity and efficiency, and mechanism, Green Chem., 21 (2019) 850–860.

[66] Y. Zou, Y. Gao, C. Xiang, H. Chu, S. Qiu, E. Yan, F. Xu, C. Tang, L. Sun, Cobalt-nickel-boron supported over polypyrrole-derived activated carbon for hydrolysis of ammonia borane, Metals, 6 (2016) 154, doi: 10.3390/met6070154.

[67] L. Xu, L. Yang, L. Shang, J. Chen, Novel Ni-based catalysts for hydrogen generation from hydrolysis of ammonia borane, IOP Conf. Ser.: Mater. Sci. Eng., 382 (2018) 022097, doi: 10.1088/1757-899X/382/2/022097.

[68] Y.-T. Li, X.-L. Zhang, Z.-K. Peng, P. Liu, X.-C. Zheng, Highly efficient hydrolysis of ammonia borane using ultrafine bimetallic RuPd nanoalloys encapsulated in porous g-C_3N_4, Fuel, 277 (2020) 118243, doi: 10.1016/j.fuel.2020.118243.

[69] R. Lu, M. Hu, C. Xu, Y. Wang, Y. Zhang, B. Xu, D. Gao, J. Bi, G. Fan, Hydrogen evolution from hydrolysis of ammonia borane catalyzed by Rh/g-C_3N_4 under mild conditions, Int. J. Hydrogen Energy, 43 (2018) 7038–7045.

[70] Y. Fan, X. Li, X. He, C. Zeng, G. Fan, Q. Liu, D. Tang, Effective hydrolysis of ammonia borane catalyzed by ruthenium nanoparticles immobilized on graphic carbon nitride, Int. J. Hydrogen Energy, 39 (2014) 19982–19989.

[71] M. Navlani-García, P. Verma, Y. Kuwahara, T. Kamegawa, K. Mori, H. Yamashita, Visible-light-enhanced catalytic activity of Ru nanoparticles over carbon modified g-C_3N_4, J. Photochem. Photobiol., A, 358 (2018) 327–333.

[72] H. Kahri, M. Sevim, Ö. Metin, Enhanced catalytic activity of monodispersed AgPd alloy nanoparticles assembled on mesoporous graphitic carbon nitride for the hydrolytic dehydrogenation of ammonia borane under sunlight, Nano Res., 10 (2016) 1627–1640.

[73] Y.-T. Li, S.-H. Zhang, G.-P. Zheng, P. Liu, Z.-K. Peng, X.-C. Zheng, Ultrafine Ru nanoparticles anchored to porous g-C_3N_4 as efficient catalysts for ammonia borane hydrolysis, Appl. Catal., A, 595 (2020) 117511, doi: 10.1016/j.apcata.2020.117511.

[74] M. Gao, Y. Yu, W. Yang, J. Li, S. Xu, M. Feng, H. Li, Ni nanoparticles supported on graphitic carbon nitride as visible light catalysts for hydrolytic dehydrogenation of ammonia borane, Nanoscale, 11 (2019) 3506–3513.

[75] J. Li, F. Li, J. Liao, Q. Liu, H. Li, $Cu_{0.4}Co_{0.6}MoO_4$ nanorods supported on graphitic carbon nitride as a highly active catalyst for the hydrolytic dehydrogenation of ammonia borane, Catalysts, 9 (2019) 714, doi: 10.3390/catal9090714.

[76] D. Li, H.-Q. Xu, L. Jiao, H.-L. Jiang, Metal-organic frameworks for catalysis: state of the art, challenges, and opportunities, EnergyChem, 1 (2019) 100005, doi: 10.1016/j.enchem.2019.100005.

[77] Y.-H. Zhou, X. Cao, J. Ning, C. Ji, Y. Cheng, J. Gu, Pd-doped Cu nanoparticles confined by ZIF-67@ZIF-8 for efficient dehydrogenation of ammonia borane, Int. J. Hydrogen Energy, 45 (2020) 31440–31451.

[78] H. Wang, F. Zheng, G. Xue, Y. Wang, G. Li, Z. Tang, Recent advances in hollow metal-organic frameworks and their composites for heterogeneous thermal catalysis, Sci. China Chem., 64 (2021) 1854–1874.

[79] D. Gao, Y. Zhang, L. Zhou, K. Yang, CuNi NPs supported on MIL-101 as highly active catalysts for the hydrolysis of ammonia borane, Appl. Surf. Sci., 427 (2018) 114–122.

[80] Y. Li, S. Li, Low-cost CuFeCo@MIL-101 as an efficient catalyst for catalytic hydrolysis of ammonia borane, Int. J. Hydrogen Energy, 45 (2020) 10433–10441.

[81] Z. Liang, X. Xiao, X. Yu, X. Huang, Y. Jiang, X. Fan, L. Chen, Non-noble trimetallic Cu-Ni-Co nanoparticles supported on metal-organic frameworks as highly efficient catalysts for hydrolysis of ammonia borane, J. Alloys Compd., 741 (2018) 501–508.

[82] K. Yang, L. Zhou, X. Xiong, M. Ye, L. Li, Q. Xia, RuCuCo nanoparticles supported on MIL-101 as a novel highly efficient catalysts for the hydrolysis of ammonia borane, Microporous Mesoporous Mater., 225 (2016) 1–8.

[83] D. Lu, G. Yu, Y. Li, M. Chen, Y. Pan, L. Zhou, K. Yang, X. Xiong, P. Wu, Q. Xia, RuCo NPs supported on MIL-96(Al) as highly active catalysts for the hydrolysis of ammonia borane, J. Alloys Compd., 694 (2017) 662–671.

[84] L. Wen, J. Su, X. Wu, P. Cai, W. Luo, G. Cheng, Ruthenium supported on MIL-96: an efficient catalyst for hydrolytic dehydrogenation of ammonia borane for chemical hydrogen storage, Int. J. Hydrogen Energy, 39 (2014) 17129–17135.

[85] M. Chen, L. Zhou, D. Lu, L. Yue, H. Ning, Y. Pan, H. Xu, W. Peng, S. Zhang, RuCo bimetallic alloy nanoparticles immobilized on multi-porous MIL-53(Al) as a highly efficient catalyst for the hydrolytic reaction of ammonia borane, Int. J. Hydrogen Energy, 43 (2018) 1439–1450.

[86] P.-Z. Li, K. Aranishi, Q. Xu, ZIF-8 immobilized nickel nanoparticles: highly effective catalysts for hydrogen generation from hydrolysis of ammonia borane, Chem. Commun., 48 (2012) 3173–3175.

[87] W. Wang, M. Liang, Y. Jiang, C. Liao, Q. Long, X. Lai, L. Liao, Nano-Co embedded in porous ZIF-67 polyhedron to catalyze hydrolysis of ammonia borane, Mater. Lett., 293 (2021) 129702, doi: 10.1016/j.matlet.2021.129702.

[88] Y.-H. Zhou, S. Wang, Z. Zhang, N. Williams, Y. Cheng, J. Gu, Hollow nickel-cobalt layered double hydroxide supported

palladium catalysts with superior hydrogen evolution activity for hydrolysis of ammonia borane, ChemCatChem, 10 (2018) 3206–3213.

[89] W. Zhao, R. Wang, Y. Wang, J. Feng, C. Li, G. Chen, Effect of LDH composition on the catalytic activity of Ru/LDH for the hydrolytic dehydrogenation of ammonia borane, Int. J. Hydrogen Energy, 44 (2019) 14820–14830.

[90] M. Paladini, G.M. Arzac, V. Godinho, M.C.J.D. Haro, A. Fernández, Supported Co catalysts prepared as thin films by magnetron sputtering for sodium borohydride and ammonia borane hydrolysis, Appl. Catal., B, 158–159 (2014) 400–409.

[91] Y. Wang, W. Meng, D. Wang, Z.R. Wang, K.L. Zou, Z.Q. Cao, K. Zhang, S.W. Wu, G.D. Li, Ultrafine cobalt-molybdenum-boron nanocatalyst for enhanced hydrogen generation property from the hydrolysis of ammonia borane, Int. J. Hydrogen Energy, 44 (2019) 23267–23276.